PAPER

Processing, thermal and mechanical behaviour of PEI/MWCNT/carbon fiber nanostructured laminate

Materials Research Express

PAPER

RECEIVED
10 October 2017

REVISED
6 November 2017

ACCEPTED FOR PUBLICATION
13 November 2017

PUBLISHED
29 November 2017

Processing, thermal and mechanical behaviour of PEI/MWCNT/carbon fiber nanostructured laminate

L F P Santos[1], B Ribeiro[2], L R O Hein[1], E C Botelho[1] and M L Costa[1]

[1] Materials and Technology Department, School of Engineering, Universidade Estadual Paulista (UNESP), Guaratinguetá, Brazil
[2] Institute of Science and Technology, Universidade Federal de São Paulo (UNIFESP), São José dos Campos, Brazil

E-mail: luiss9406@gmail.com

Keywords: multiwalled carbon nanotube, polyetherimide, thermal analysis, mechanical properties

Abstract

In this work, nanostructured composites of polyetherimide (PEI) with addition of functionalized multiwall carbon nanotube (MWCNT) were processed via solution mixing. After processing, these nanocomposites were evaluated by thermogravimetry (TGA), dynamic-mechanical analysis (DMA), scanning electron microscopy (SEM) and atomic force microscopy (AFM). Subsequently, the nanocomposite was processed with carbon fibers by using hot compression molding. In order to evaluate interlaminar fracture strength, the processed laminates were mechanically evaluated by interlaminar shear strength (ILSS) and compression shear test (CST). Also, the Weibull distribution was employed to help in the statistical treatment of the data obtained from the mechanical tests. With regards to the fracture of the specimens, optical microscopy was used for the evaluation of the material. The addition of 1 wt% of MWCNT in the polymer matrix increased both thermal stability and viscoelastic behavior of the material. These improvements positively impacted the mechanical properties, generating a 16% and 58% increase in the short-beam strength and apparent interlaminar shear, respectively. In addition, it can be verified from morphological analysis of the fracture a change in the failure mode of the laminate by the incorporation of MWCNT. This behavior can be proven from CST test where there was no presence of the shear force by compression.

1. Introduction

The use of carbon fiber-reinforced polymer composites (CFPC) has been growing due its excellent strength-to-weight and stiffness-to-weight ratio, which allows its use in a variety of high-performance applications, especially in the aerospace industry [1, 2]. Among them, thermoplastic composites with high temperature applications stand out due mainly to its recyclability, high chemical resistance to solvent and radiation, reprocessing, and consequently generate laminates with improved mechanical properties (high level of toughness, strength, stiffness and resistance to fatigue) [3, 4]. In addition to this growing use, there is also a need to incorporate the concept of multifunctional materials, in other words, multipurpose materials that do not only have the mechanical support function but which combine thermal, electrical, magnetic, optical features [4].

Within this context are the nanostructured composites, particularly those constituted with the addition of carbon nanotubes (CNT), which has increasingly gained importance in academic community, since the introduction of this nanomaterial has shown promising results [5–7]. The CNTs possess remarkable characteristics, such as high aspect ratio (~1000), low density (2.0 g cm^{-3}) and excellent mechanical, thermal and electrical properties [8–10]. Therefore, the addition of this nanoparticles as a reinforcement in polymer composites gives the material not only mechanical but also thermal and electrical improvements [4, 11, 12].

Although the incorporation of CNTs in polymeric matrices as reinforcements is not a new concept, the formation of bundles and agglomerates are still the major bottlenecks of their utilization in polymer composites. Due to van der Waals forces acting on them, high surface area and high aspect ratio, the agglomeration of the nanoparticles generate non-homogeneous composites, which results in deterioration of the final properties of the material, thus limiting its applications [13–15]. Therefore, several methods have been developed in order to improve the dispersion of the carbon nanotubes in the polymer matrix, as an example, the chemical

functionalization that consists of the addition of functional groups in CNT surface and the physical functionalization that represents the use of surfactants as dispersing agents [16, 17].

As previously mentioned, the aerospace sector has a particular interest in CFPC, but it is known that a factor to consider and that limits the life of the material is related to the failure mechanisms presented that are complex due to the anisotropy and heterogeneity of the material [19]. Among the faults that a composite can present, the interlaminar fracture is potentially one of the main, due to the absence of the orthogonal reinforcement to the plane of the fibers [20]. Interlaminar failure, better known as delamination, can introduce a significant reduction of structural stiffness without external signs of damage, resulting in a catastrophic failure [21]. The interlaminar properties of the laminated composites depend on the characteristics of the matrix and the interface, which represents an important source of weakness and generates shear stresses [22]. The use of nanoparticles is an alternative to improve the hardness of the matrix, consequently impacting a significant increase in fracture resistance and extending the life of the material [2]. Previous studies [23] show the addition of CNT generated increases in delamination resistance and out-of-plan properties have been shown to improve through interactions between propagation cracks and CNTs through different mechanisms, such as CNT debonding, cracks deflection and crack pinning.

The polymer matrix used in this work was poly (ether-imide) (PEI), which is an engineering thermoplastic widely used in aircraft due to its properties such as high mechanical strength, high stiffness, high glass transition temperature (210–220 °C), good resistance to flammability and easy processability [5, 9, 18]. According to the literature [24] the incorporation of CNT into neat PEI is related to a 5% increase in the glass transition temperature (T_g) of the material, an increase of approximately 10% in the initial, final and maximum degradation temperature and an increase of about 7% in tensile strength. According to [25] the incorporation of CNT generated a 3% increase in Tg, an increase of approximately 4% in initial and maximum degradation temperature and a 5% increase in tensile strength and tensile modulus.

The present work aims to present the processing of nanostructured composites of PEI/MWCNT/CF as well as their characterization from thermal analysis and morphological analysis to verify the dispersion of CNT_S. The laminates were processed by hot compression molding technique and evaluated by mechanical tests, such as interlaminar shear strength (ILSS) and compression shear test (CST). Finally, a fractographic analysis was performed in order to study the failure of the laminates.

2. Experimental

2.1. Materials

PEI, used as the matrix in the present work, was supplied by SABIC's Innovative Plastics Company (ULTEM 1010). This material presents the following properties: $d_{25\,°C} = 1.28\,g\,cm^{-3}$ and $T_g \sim 217\,°C$. In order to promote the consolidation of the composites, it was used plain weave carbon fiber fabrics supplied by the American company Hexcel Composites, containing 3000 monofilaments per cable, a specific mass of $1.77\,g\,cm^{-3}$ and thickness around 0.17 mm. Functionalized MWCNT used as nanoreinforcements, were supplied by Cheap Tubes with average diameter of their walls about 8–15 nm, length between 10–50 μm and $d_{25\,°C} = 2.1\,g\,cm^{-3}$. The surfactant (Triton X-100) provided by Labsynth is a viscous, yellowish colored liquid with pH between 6.0 and 8.0, with boiling temperature around 270 °C and density between 1.064 and $1.067\,g\,cm^{-3}$.

2.2. Fourier transform infrared spectrocopic (FTIR) analysis

The FTIR analysis was perfomed using a Fourier transform spectrometer (Spectrum 100, PerkinElmer) in the wavenumbers range of 650–4000 cm^{-1} and resolution of 40 cm^{-1} to characterize the functionalized MWCNTs.

2.3. Processing of neat PEI and PEI/MWCNT films

The preparation of neat PEI film was conducted in two main steps: Firstly, 10 g of the PEI polymer matrix in pellets was dispersed into 250 ml of methylene chloride on a magnetic stirrer for 30 min. Subsequently, the solution was placed in aluminum mold (30 × 30) cm in size and then carried in a vacuum oven at 40 °C for 3 h in order to remove the solvent and obtain the film. The vacuum oven used was of the Vacucell brand and model VUK/VU 55. The temperature of 40 °C has been chosen because it is close to the boiling temperature of the solvent.

The process of obtaining the PEI/MWCNT composite film was performed in four steps: (1) 0.1 g of MWCNT, which corresponds to 1% by weight based on the mass of the polymer and 0.5 g of Triton X-100 were dispersed in 50 ml of methylene chloride for 30 min with the aid of the Sonics & Materials ultrasonic tip model VC 750; (2), 10 g of PEI in pellets was dispersed into 200 ml of methylene chloride for 30 min in the magnetic stirrer; (3) both solutions obtained in the first and second stages were mixed and taken to the ultrasonic tip for another 40 min; and (4) finally, the solution of PEI, MWCNT, methylene chloride and Triton X-100 was placed in an aluminum mold (30 × 30)cm in size and was oven-dried at 40 °C for 3 h to remove the solvent and obtain the film of PEI/MWCNT composite film. The Triton X-100 used consists of a surfactant that is intended to aid in the stability

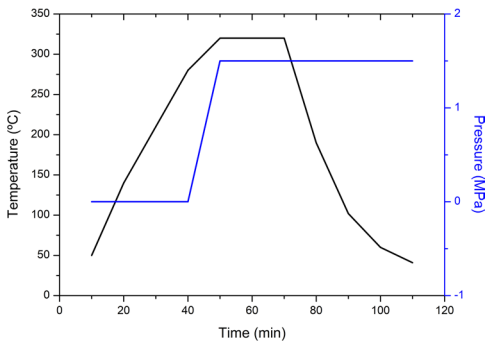

Figure 1. Processing cycle by hot compression molding.

of the dispersion of the carbon nanotubes. In steps 1 and 2, the beaker containing the respective solutions was placed into a container with ice to avoid evaporation of the solvent.

2.4. Characterization of the polymer matrix by thermal analysis

The thermogravimetric analyzes (TGA) were performed using the equipment of SII Nanotechnology—Seiko Model TG/DTA 6200. Samples of about 5 mg were placed in platinum pan and alumina was used as reference material. Then samples were heated at a rate of 10 °C min^{-1}, under nitrogen flow of 50 ml min^{-1} from temperature range of 25–1000 °C.

Dynamic-mechanical analyzes (DMA) were performed in a SII Nanotechonology—SEIKO model DMS 6100 according to the following parameters: tensile mode, nitrogen atmosphere under flow of 100 ml min^{-1}, oscillation amplitude of 10 μm, frequency of 1 Hz, heating rate of 3 °C min^{-1} and temperature range from 25 °C to 250 °C. The specimens were cut into the dimensions of (50 × 10 × 0.1) mm.

2.5. Processing of PEI/FC and PEI/MWCNT/FC composites laminates

The PEI/FC and PEI/MWCNT/FC laminates were processed through hot compression molding technique, from alternating stacking of 12 layers of fabrics and 16 layers of polymer film into a stainless-steel mold, previously prepared with release agent. The processed laminates have a thickness of 3 mm and a matrix/reinforcement volumetric content of 50/50 (v/v). The consolidation of the material was performed in a hot compression molding equipment (Carver model CMG100H-15-X) at 320 °C under pressure around 1.5 MPa for 20 min. The thermal cycle (figure 1) was optimized to minimize the formation of internal pores and to improve the impregnation between fabrics and polymer film.

2.6. Interlaminar shear strength (ILSS)

The ILSS tests were performed according to ASTM D2344/D2344M-16 standard. The dimensions of the test specimens are (18 × 6 × 3) mm and 10 specimens were used for each material. The tests were performed in a universal Shimatzu mechanical test machine (Autograph AG-X series) and the parameters used were: speed of 1.0 mm min^{-1} and load cell of 10 KN. In order to calculate the short-beam strength (Fsbs), equation (1) was employed, where P is the maximum load observed during the test, b measured specimen width and h measured specimen thickness.

$$F^{sbs} = \frac{0.75\,P}{bh}. \tag{1}$$

2.7. Compression shear test (CST)

The CST was developed by the researchers Schneider, Lauke and Beckert at the Institute of Polymer Research Dresden in Germany [26]. This test consists of the generation of a direct shear load along the interlaminar interface and forces the separator to break in pure shear. The distribution of the shear stress is almost uniform across the thickness with two peaks close to the edges of the loading surface [26–28]. To perform this test, 5 specimens with dimensions of (10 × 10 × 3) mm were used, the test speed was 0.25 mm min^{-1} and 10 KN load cell. A universal Shimatzu mechanical test machine, (Autograph AG-X series), was used to perform these tests. In this test the apparent interlaminar shear stress is calculated by equations (2) and (3), where σ_{app} is the apparent interlaminar shear stress in MPa, P_{eff} is the effective load in Kgf, P_{tot} is the load applied in Kgf, z is the horizontal distance of the pivot of the movable arm in mm, R_d is the radius of movable arm in degrees and d_i is the half-width of the sample which is subjected to the compression force in mm.

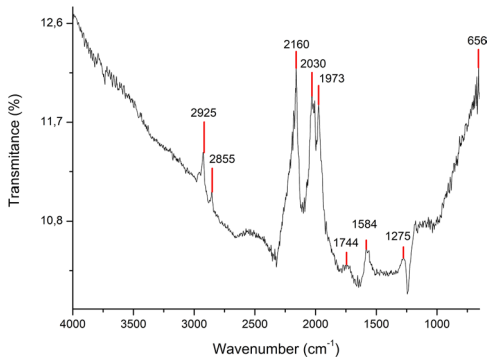

Figure 2. FTIR spectrum COOH modified MWCNTs.

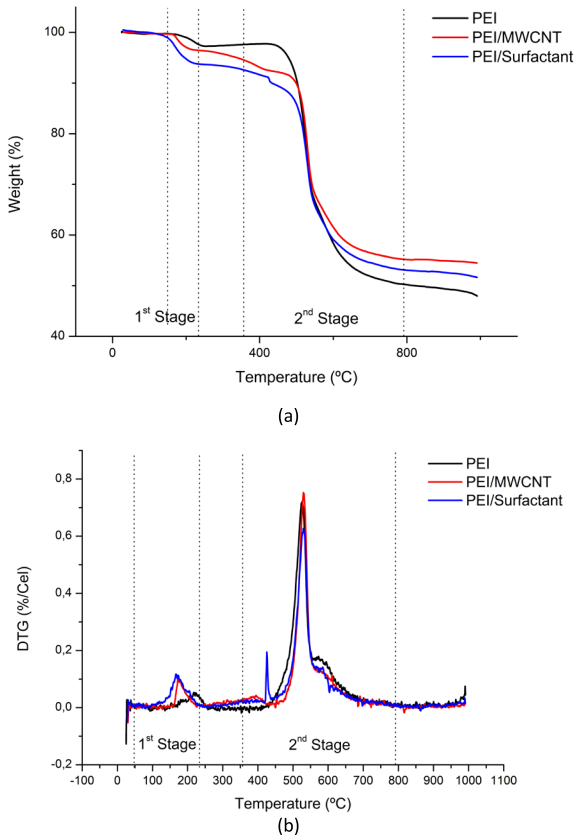

Figure 3. Representative curves of thermogravimetric analysis: (a) TGA; (b) DTG for the PEI; PEI/MWCNT and PEI/Surfactant films.

$$\sigma_{\text{app}} = \frac{P_{\text{eff}}}{(l \times b)} \tag{2}$$

$$P_{\text{eff}} = \frac{P_{\text{tot}} \times z}{(R_{\text{d}} + d_i)}. \tag{3}$$

2.8. Morphological analysis

The morphological analysis was evaluated in two stages. The first step is to verify the dispersion of MWCNTs in the polymer matrix, so scanning electron microscopy (SEM) and atomic force microscopy (AFM) were employed. SEM was performed on a Zeiss microscope, model EVO LS-15 with tungsten filament. The samples were fractured with a pair of scissors, placed in the sample port of alumina on a carbon double-face tape, a nitrogen jet was applied to clean the samples and finally the samples were covered with a thin layer of gold. The AFM was performed on a Shimadzu microscope, model SPM-9600. The samples were fractured with scissors, cleaned with a jet of nitrogen and placed on the aluminum sample port. In the second stage, the morphological analysis had

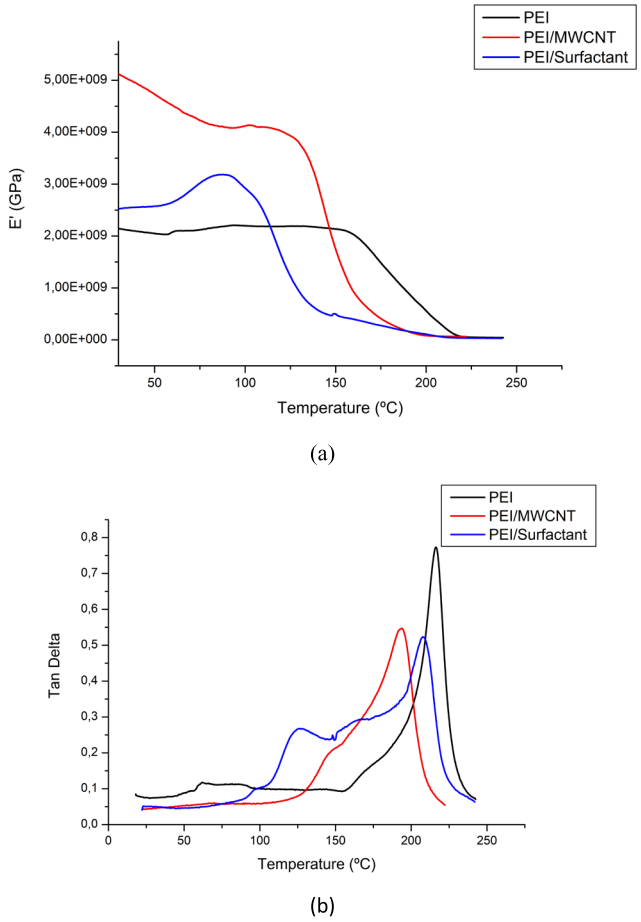

Figure 4. Viscoelastic behavior determined by DMA of PEI, PEI/surfactant and PEI/MWCNT films.

the objective of analyzing the fracture aspect of the specimens tested. In this step, an optical microscope (OM) Zeiss Axio Imager Z2m equipped with incandescent halogen-tungsten lamp and digital camera AxioCam ICc3 of Zeiss were used.

3. Results and discussions

The functionalization of MWCNT by the addition of the COOH group was confirmed by formed peaks related to the existence of several functional groups present in MWCNTs, as shown in figure 2. Taking as reference the work [24, 25, 29] it can be observed that the bands referring to the carbonyl group (C=O) of the sample is broad with a peak around 1275 cm^{-1}. In the spectrum of wavenumber ~1000 cm^{-1} it was verified the presence of a weak stretching belonging to the C–C bonds. It is also noted that distinct peaks formed at 1744 cm^{-1} (asymmetric stretching) and 1584 cm^{-1} (symmetric stretching), such peaks are related to the stretching absorption of the carboxylic acid (C=O). The peaks between 2160 cm^{-1} and 1973 cm^{-1} can be associated with the presence of O−H stretch from strongly hydrogen-bonded −COOH. In addition, peaks at 2925 and 2855 cm^{-1} may be associated respectively to free hydroxyl groups and the O–H stretch from carboxyl groups (O=C–OH and C–OH). Therefore, after this analysis it was possible to verify the efficiency of the functionalization process of the carbon nanotubes due to the presence of the carboxyl groups. According to previous works [24, 25], the incorporation of such functional groups makes easy the formation of hydrogen bonds of the CNT with electronegative atoms (–O and –H) present in the polymer chain of the PEI and also helps to obtain a better interfacial interaction between the polymer and the CNT. Also, it worth to mention that the as-prepared MWCNT were purified by the manufacturer and the catalytic metallic particles were possibly removed during the process. Thus, the incorporation of carboxylic groups in these MWCNT was confirmed by FT-IR.

The thermal behavior of the neat PEI, PEI/MWCNT and PEI/Surfactant is shown in figure 3. It is observed that both exhibit a similar behavior and two stages of decomposition. In the first stage of degradation between 150 °C and 300 °C the evaporation of the volatile compounds present in the materials occurs, in case of PEI evaporation of the methylene chloride solvent and for the PEI/MWCNT and PEI/Surfactant evaporation of the methylene chloride and the surfactant Triton X-100. In the second stage of degradation, the addition of the nanotubes

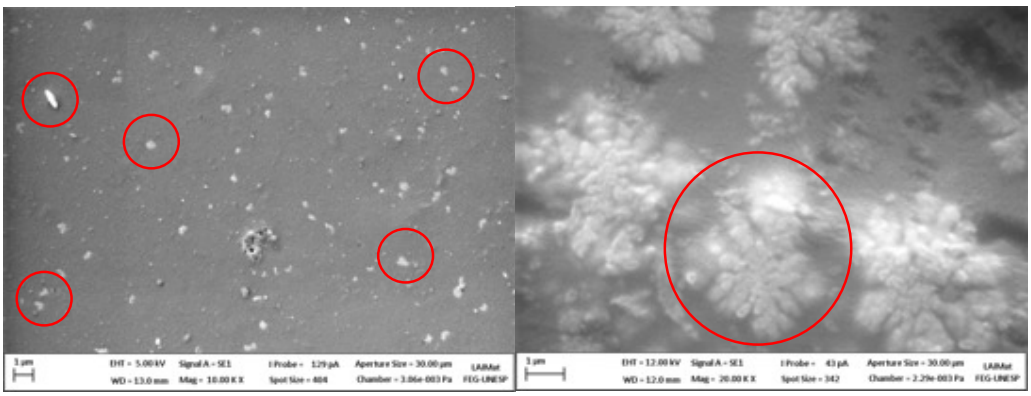

(a) (b)

Figure 5. SEM images of PEI/MWCNT nanocomposite with 1 wt%: (a) general aspect; (b) pseudo crystals morphology view.

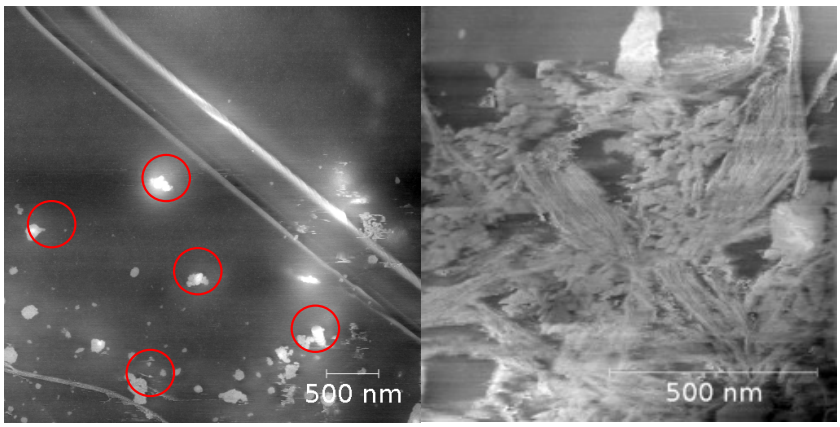

(a) (b)

Figure 6. Amplitude views for Phase mode AFM image of PEI/MWCNT nanocomposite with 1 wt% (a) crystal particles dispersion in amorphous polymer chain at 4.0 μm by 4.0 μm field view; (b) detail of pseudo crystals formation.

was responsible for increasing the initial temperature (T_i), 427 °C for neat PEI and 460 °C for PEI/MWCNT and the addition of surfactant reduces the T_i for 418 °C. Also, it can be noted a 6 °C increase in T_{max} (peak temperature in DTG), which suggests an improvement in thermal stability of the polymer matrix after the addition of MWCNT and for PEI/Surfactant it can be noted a 3 °C increase in T_{max}. The observed behavior for the PEI/MWCNT may be associated to the following factors: good dispersion and suitable interaction between PEI and MWCNT, which makes difficult to diffuse degradation products, delaying thermal decomposition; strong interaction through the π–π bonds that restricts the mobility of the polymer chain and increases the barrier effect; the high thermal conductivity of the MWCNT facilitates the dissipation of heat inside the composite [7, 11, 17]. The final temperature of degradation (T_f) for both cases is 750 °C, but it is verified that the residue weight for the neat PEI, PEI/MWCNT and PEI/Surfactant composite were respectively 48%, 55% and 51%. This fact is expected since in the material with MWCNT addition there is a greater amount of carbon specimens.

The viscoelastic behavior of the films is shown in figure 4. From the curve of the storage modulus (E') and taking as reference the temperatures of 30 °C and 80 °C, it is observed that the values of E' for PEI and for PEI/MWCNT composite were 2.2 and 5.2 GPa at 30 °C, respectively, representing a 136% increase by the incorporation of MWCNT in PEI. According to the literature [17, 30], the improvement in the viscoelastic properties of the polymer matrix by the addition of the nanoreinforcements may be associated mainly with the adequate dispersion of the CNT during the processing of the PEI/MWCNT film, optimizing the reinforcement/matrix interface. Similarly, at 80 °C, the storage modulus values of the polymer matrix and its nanostructured composite were 2.1 and 4.2 GPa, representing a 100% increase in this condition. Also in the E' curve it is verified that for the PEI/surfactant line there is an increase of the module starting at 60 °C, this fact can be associated to the use of the surfactant that from this temperature begins to be eliminated from the sample and, therefore, causing increase of the module from this temperature.

Table 1. ILSS and CST measurements and parameters obtained from the Weibull distribution.

Sample	ILSS (MPa)	B	R
PEI/FC	86.27 ± 6.89	11.39	0.948 84
PEI/MWCNT/FC	100.48 ± 6.99	13.61	0.968 53
Sample	CST (MPa)	β	R
PEI/FC	3.79 ± 0.70	3.331 92	0.774 98
PEI/MWCNT/FC	6.02 ± 0.62	6.691 30	0.990 60

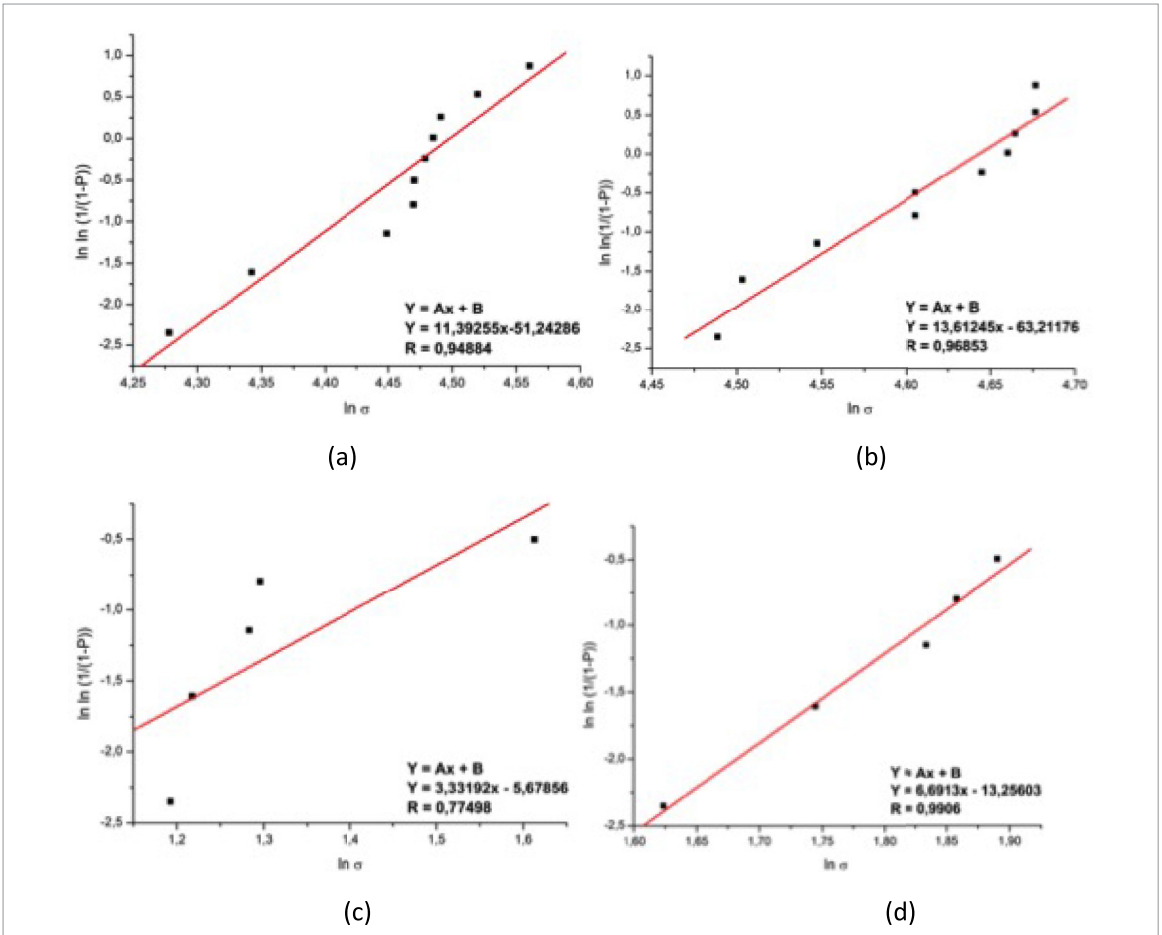

Figure 7. Weibull distribution results: (a) ILSS for PEI/FC; (b) ILSS for PEI/MWCNT/FC; (c) CST for PEI/FC; (d) CST for PEI/MWCNT/FC.

The glass transition temperature of the matrix and the nanostructured composite was obtained from the peak of the tan δ curves. As can be observed, pure PEI has a T_g of 216 °C, which is consistent with that values reported in the literature [24, 25]. In the case of the PEI/MWCNT film, a reduction in T_g was observed. According to previous works [28, 30], the reduction of the glass transition temperature by the use of surfactants during the dispersion of nanoparticles may be associated with a plasticizer effect in the matrix, showing an increase in the mobility of the polymer chains and, consequently, a reduction in the T_g of the composite.

The morphology of the PEI/MWCNT nanocomposite was evaluated by SEM and AFM. In figure 5(a) it is observed that the MWCNT dispersion in the polymer matrix was relatively homogeneous, however there are small regions with agglomerates, which are due to the van der Walls interactions, these regions are indicated by the red arrows. In addition, such dispersion suggests a good adhesion between MWCNT and the polymer matrix, indicating good wettability between them [31]. It is important to emphasize that the functionalization of MWCNT with the carboxyl group (COOH) and the use of Triton X-100 surfactant helps to obtain a more homogeneous structure [16, 24]. In figure 6(b) it is observed that the addition of MWCNT in some regions generated an ordering of the amorphous polymer chain, consequently forming pseudo crystals [32]. The presence of pseudo crystals alters the morphology of the amorphous polymer chain, acting on the macroscopic properties of the nanocomposites, especially the mechanical. Figure 5 shows the micrographs obtained from the AFM. Figure 5(a) also shows a homogeneous dispersion of MWCNT and figure 5(b) shows the presence of pseudo crystals, both images according to the information obtained by MEV.

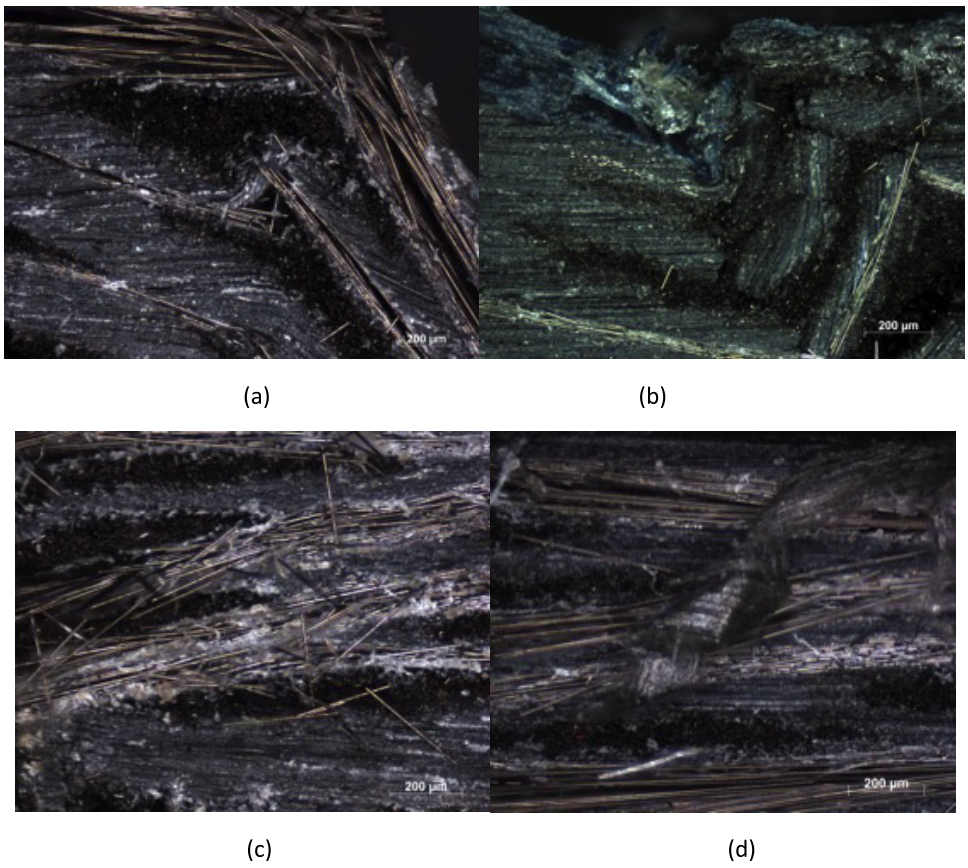

Figure 8. Light microscopy of the fracture region: (a) ILSS for PEI/FC; (b) ILSS for PEI/MWCNT/FC; (c) CST for PEI/FC; and (d) CST for PEI/MWCNT/FC.

Table 1 presents the short-beam strength results obtained by ILSS and the apparent interlaminar shear obtained by CST. Analyzing the results, it was observed that the short-beam strength increased by 16% and the apparent interlaminar shear increased by 58% when MWCNT was added to the polymer matrix. Also, it can be noted that there was a significant increase in the apparent interlaminar shear, but despite that increase the values found are below the expected, which may be the absence of the shear force by compression load.

In order to aid in the analysis of the data it is essential to use a statistical treatment, so in this case the Weibull distribution was employed. The Weibull distribution works with the probability of the material, after the load application, to resist or not, even if the load is below the mean of the conventional strength limit of the material. Material rupture results from the occurrence of failures during this process and the Weibull distribution will quantify this probability. For the determination of the coefficients that rule the distribution of Weibull frequencies, it was constructed the Cartesian axes a set of points whose coordinates are, in the axis of the abscissas, the neperian logarithm of the studied property, that is, $x = \ln \sigma$ and in the axis of the ordinates, according to equation (4), where P is the median rank function [33].

$$y = \ln\left[\ln\left(\frac{1}{1-P}\right)\right]. \tag{4}$$

From the linearization of the points, it was obtained the equation of the line and from it was calculated the Weibull (β) modulus, which is indicated by the number that accompanies the parameter 'x', the information obtained is shown in table 1 and figure 7. When analyzing the values of β for both tests it is verified that the composites with MWCNT present a larger Weibull modulus, therefore they present less dispersion of the results. This lower dispersion of the results and increase in the load values observed is due probably to the increase in matrix hardness, a good interface between the polymer and MWCNT and also the plasticizer effect generated by the use of the surfactant favored the impregnation of the polymers in the fibers during the hot compression molding process. Such behavior was observed from the characterization by thermal analysis of the polymer matrix, such improvements favor the reduction of fracture toughness. The determination factor or adjustment parameter (R) indicates how well the points are adjusted to the straight line, so when closer to 1, greater reliability in the results is obtained. Again, it is verified that for the mechanical tests for the composites with addition of MWCNT they present greater reliability.

Figure 8 shows the micrographies of the fracture region of the ILSS and CST samples. The fracture for the ILSS specimens occurred in the central region of the specimen, that is, at the site of load application and after the fracture the specimen was in V-shape. Comparing figures 8(a) and (b), it is observed that the PEI/FC laminate underwent a translaminar fracture and apparently in a fragile form, whereas the PEI/MWCNT/FC laminate also presented a translaminar fracture, but appears to have undergone flexion before fracture, suggesting that it is fracture was a bit tricky. As previously stated, the specimens in the CST test did not undergo compression shear but rather a flexion, so the fracture of the specimen is in the region where the specimen was supported and affixed to the loading, as presented in figures 8(c) and (d). For both laminates the fracture is similar.

4. Conclusions

In this work, the processing of PEI/MWCNT nanocomposites and their characterization by thermal analysis and later the processing of the laminates with carbon fibers and analysis of the interlaminar fracture strength were analyzed. The processing of the nanocomposite by solution mixture, since the thermal analyzes of TGA and DMA and the microscopies performed have shown that the MWCNT were well dispersed in the polymer matrix, therefore, improving the thermal stability and the viscoelastic properties of the material. The use of the Triton X-100 surfactant generated a plasticizing effect on the polymer matrix reducing its T_g by approximately 22 °C and, consequently, increased wettability of the polymer matrix, favored impregnation in the carbon fibers and resulted in a material with a stronger consolidation after processing through hot compression molding. On the mechanical behavior of the laminates studied, it was verified that the addition of MWCNT improved the fracture resistance, in the case of ILSS there was an increase of 16% and in the case of the CST an increase of 58%, although this test presented values lower than expected by not the presence of the compression shear force but rather a bending force. From the Weibull distribution, it was verified that the laminate with MWCNT presents a lower dispersion of the results and greater reliability. Finally, by analyzing the micrographs of the region of the fracture of the samples, it was verified that the presence of MWCNT in the laminate made the fracture a slightly ductile when submitted to the ILSS test.

Acknowledgments

The authors acknowledge financial support received from Sao Paulo Research Foundation (FAPESP) under project number 2016/12810-5 and National Council for Scientific and Technological Development (CNPq), both from Brazil.

ORCID iDs

L F P Santos https://orcid.org/0000-0002-5089-1089

References

[1] Kwon Y J, Kim Y, Jeon H, Cho S, Lee W and Lee J U 2017 Graphene/carbono nanotube hybrid as a multi-functional interfacial reinforcement for carbono fiber-reinforced composites *Composites* B **122** 23–30
[2] Srivastava V K, Gries T, Veit D, Quadflieg T, Mohr B and Kolloch M 2017 Effect of nanomaterial on mode I and mode II interlaminar fracture toughness of woven carbon fabric reinforced polymer composites *Eng. Fract. Mech.* **180** 73–86
[3] Gabrion X, Placet V, Trivaudey F and Boubakar L 2015 About the thermomechanical behaviour of a carbon fiber reinforced high-temperature thermoplastic composites *Composites* B **95** 386–94
[4] Dubary N, Taconet G, Bouvet C and Vieille B 2017 Influence of temperature on the impact behaviour and damage tolerance of hybrid woven-ply thermoplastic laminates for aeronautical applications *Compos. Struct.* **168** 663–74
[5] Ferreira A D B L, Nóvoa P R O and Marques A T 2016 Multifunctional material system: a state-of-the-art review *Compos. Struct.* **151** 3–35
[6] Rahmat M and Hubert P 2011 Carbon nanotube-polymer interactions in nanocomposites: a review *Compos. Sci. Technol.* **72** 72–84
[7] González I and Eguiazábal J I 2013 Widely dispersed PEI-based nanocomposites with nulti-wall carbon nanotubes by blending with a masterbatch *Composites* A **53** 176–81
[8] Quigley J P, Herrington K and Bair D G 2014 Enhanced electrical properties of polycarbnate/carbon nanotube nanocomposites prepared by a supercritical carbon dioxide aided melt blending method *Polymer* **55** 6167–75
[9] Mittal G, Dhand V, Rhee K Y, Park S J and Lee W R 2014 A review on carbon nanotubes and graphene as fillers in reinforced polymer nanocomposites *J. Ind. Eng. Chem.* **21** 11–25
[10] Vorobei A M, Pokrovsky O I, Ustinovich K B, Parenago O O, Savilov S V, Lunin V V and Novotortsev V M 2016 Preparation of polymer-multi walled carbon nanotube composute with enhanced mechanical properties using supercritical antisolvent precipitation *Polymer* **95** 77–81
[11] Tunckol M, Hernandez E Z, Sarasua J R, Durand J and Serps F 2013 Polymerized ionic liquid functionalized multi-walled carbon nanotube/polyetherimide composites *Eur. Polym. J.* **49** 3370–7
[12] Sairajan K K, Aglietti G S and Mani K M 2016 A review of multifunctional structure technology for aerospace applications *Acta Astronaut.* **120** 30–42

[13] Spitalsky Z, Tasis D, Papagelis K and Galiotis C 2010 Carbon nanotube-polymer composites: chemistry, processing, mechanical and electrical properties *Prog. Polym. Sci.* **35** 357–401
[14] Roy N, Sengupta R and Bhowmick A K 2012 Modifications of carbon for polymer composites and nanocomposites *Prog. Polym. Sci.* **37** 781–819
[15] He D, Fan B, Zhao H, Yanh M, Wang M, Bai J, Li W, Zhou X and Bai J 2017 Multifunctional polymer composites reinforced by carbon nanotubes-Alumina hybrids with urchin-like structure *Mater. Today Commun.* **11** 94–102
[16] Goh P S, Ng B C, Ismail A F, Aziz M and Sanip S M 2010 Surfactant dispersed multi-walled carbon nanotube/polyetherimide nanocomposite membrane *Solid State Sci.* **12** 2155–62
[17] Ferreira F V, Francisco W, Menezes B R C, Cividanes L S, Coutinho A R and Thim G P 2015 Carbon nanotube functionalized with dodecylamine for the effective dispersion in solvents *Appl. Surf. Sci.* **357** 2154–9
[18] Wang H 2009 Dispersing carbon nanotubes using surfactants *Curr. Opin. Colloid Interface Sci.* **14** 364–71
[19] Dong H, Li Z, Wang J and Karihaloo B L 2016 A new fatigue failure theory for multidirectional fiber-reinforced composite laminates with arbitrary stacking sequence *Int. J. Fatigue* **87** 294–300
[20] Reis J F, Abrahao A B M, Costa M L and Botelho E C 2016 Avaliação da resistência interlaminar do compósito PEI/Fibras de Carbono soldado pelo método de resistência elétrica *Soldagem Inspeçao* **21** 387–404
[21] Zabala H, Aretxabaleta L, Castillo G and Aurrekoetxea J 2016 Dynamic 4 ENF test for a strain rate dependent mode II interlaminar fracture toughness charaterization of unidirectional carbon fiber epoxy composites *Polym. Test.* **55** 212–8
[22] Nash N H, Young T M and Stanley W F 2016 The influence of a thermoplastic toughening interlayer and hygrothermal conditioning on the mode-II interlaminar fracture toughness of carbon/benzoxazine composites *Composites* A **81** 111–20
[23] Díez-Pascual A M, Naffakh M, Marco G, Gómez-Fatou M A and Ellis G J 2014 Multiscale fiber-reinforced thermoplastic composites incorporating carbon nanotubes: a review *Curr. Opin. Solid State Mater. Sci.* **18** 62–80
[24] Pitchan M K, Bhowmik S, Balachandran M and Abraham M 2016 Effect of surface functionalization on mechanical properties and decomposition kinetics of high performance polyetherimide/MWCNT nano composites *Composite* A **90** 147–60
[25] Pitchan M K, Bhowmik S, Balachandran M and Abraham M 2017 Processo optimization of functionalized MWCNT/polyetherimide nanocomposites for aerospace application *Mater. Des.* **127** 193–203
[26] Schneider K, Lauke B and Beckert W 2001 Compression shear test (CST)—a convenient apparatus for the estimation of apparent shear strength of composites materials *Appl. Compos. Mater.* **8** 43–62
[27] Botelho E C and Rezende M C 2002 Caracterização mecânica de compósitos de poliamida/fibra de carbono via ensaios de cisalhamento interlaminar e de mecânica da fratura *Polímeros: Ciência e Tecnologia* **12** 153–63
[28] Rojas J A, Santos L F P, Costa M L, Ribeiro B and Botelho E C 2017 Moisture na temperature influence on mechanical behaviour of PPS/buckpapers carbon fiber laminates *Mater. Res. Express* **4** 075302
[29] Atieh M A, Bakather O Y, Al-Tawbini B, Bukhari A A, Abuilaiwi F A and Fettouhi M B 2010 Effect of carboxylic functional group functionalized on carbon nanotubes surface on the removal of lead from water *Bioinorg. Chem. Appl.* **2010** 1–9
[30] Velasco-Sants C, Martinez-Hernandez A L, Fisher F, Ruoff R and Castaño V M 2003 Dynamical-mechanical and thermal analysis of carbon nanotube-methyl-ethyl methacrylate nanocomposites *J. Phys. D: Appl. Phys.* **36** 1423–8
[31] Liu T, Tong Y and Zang D W 2006 Preparation and characterization of carbon nanotube/polyetherimide nanocomposite films *Compos. Sci. Technol.* **67** 406–12
[32] Liang Y Y, Xu J Z, Liu X Y, Zhong G J and Li Z M 2013 Role of surface chemical groups on carbon nanotubes in nucleation for polymer crystallization: Interfacial interaction and steric effect *Polymer* **54** 6479–88
[33] Rabahi R F and Neto F L 2016 Analysis of the strength of synthetic marble beams through the statistical distribution of Weibull *Matéria* **21** 542–51